DEVELOPMENT OF AN AEROENGINE SECONDARY AIR SYSTEM EMPLOYING VORTEX REDUCERS

M. Pfitzner* and W. Waschka+

Rolls-Royce Deutschland, Eschenweg 11, D-15827 Dahlwitz, Germany

Keywords: *Aeroengine gas turbine, secondary air system, vortex reducer*

Abstract

Modern aeroengine designs use a secondary air system to cool the rotor discs and to seal cavities between rotor and stator parts. Air is bled from the inner compressor annulus to internal parts of the engine. A vortex reducer system can reduce pressure losses along the flow path due to high swirl. The paper describes two vortex reducer systems, tubed and tubeless, both employed in BR700 aeroengines in service. The characteristics and merits of both systems are discussed and test results from rig and engine tests are shown.

1 Introduction

The basic goal of the secondary internal air system in aeroengines are to absorb the heat of the highly thermally loaded turbine discs, to prevent hot gas ingestion from the main turbine gas path into the cavities between the turbine discs and to seal the bearing chambers against oil leakage. The required cooling and sealing air mass flow is bled off from the HP compressor and is led to the turbine and to the bearing chambers either externally through pipes or internally through passages inside of the rotating components. The second option of internal bleed provides the higher integrity route and the higher bleed air purity and thus is preferable for safety reasons. The flow path in a typical internal bleed configuration of the air system is shown in fig. 1.

In most engine application the maximum allowable bleed air temperature is purely defined by the life targets for rotating components. Since the bleed off-take station in the compressor is defined by the required source pressure rather than by air temperature limits, it is important to optimise the pressure losses through the internal air system passages, bends and rotating disc holes. There is a large temperature benefit if there is the potential to move the bleed off-take one stage upstream.

2 Symbols and Abbreviations

a,b	Index (outflow, inflow of cavity)
A,B,C,D,E,F	Index (Radial positions in vortex reducer flow path)
a_v	Enthalpy change from Euler eq.
c_p	Specific heat
$C_{eff} = V_W / \Omega r_b$	Eff. swirl ratio into radial cavity
$C_W = m / \mu \cdot r_b$	Mass flow function
HP	high pressure
κ	Isentropic exponent
LP	low pressure
$\lambda = C_W / \mathrm{Re}_W$	Non-dimensional mass flow
m	Vortex reducer inlet mass flow
NH	HP shaft rotational speed
Δp	Cavity Pressure drop
p	Static pressure
P	Total pressure
$\mathrm{Re}_W = \Omega \cdot r_b{}^2 / \upsilon$	Rotational Reynolds Number
r	Radius
ρ	Density
t	Static gas temperature
T	Total gas temperature
V_W	Whirl velocity
ν	Kinematic viscosity
Ω	Rotational disc speed

* Michael.Pfitzner@rolls-royce.com
+ now at MTU München, Dachauer Str. 665, D-80995 München, Germany, Walter.Waschka@muc.mtu.dasa.de

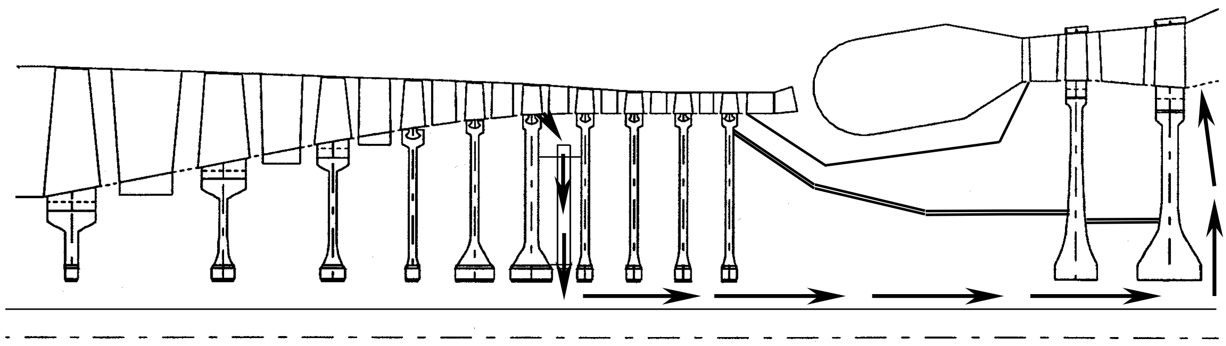

Figure 1: Internal bleed air system scheme

3 Vortex Reducer Systems

3.1 Need for Vortex Reducer Systems

One key element of the internal air system with respect to pressure losses is the radial passage between co-rotating discs. Air taken from the compressor inner wall features a high degree of swirl, which increases dramatically if the air is allowed to freely flow between the discs to a much smaller radius. This would cause large pressure losses and accordingly the flow capacity of such a design would be quite small. This can be understood by considering the pressure drop Δp of incompressible flow in a cavity,

$$\Delta p = P\_total, inlet - p\_static, outlet$$

For a free vortex in a cavity with inlet radius r_b and outlet radius r_a, the pressure drop is proportional to

$$\Delta p \sim (\rho \cdot V_W{}^2 \cdot / 2) \cdot ((r_b / r_a)^2 - 1) \qquad (1)$$

Clearly, at a given entry swirl velocity V_W the cavity pressure drop Δp becomes very large as the ratio of exit and entry radii $r_{a/}\, r_b \rightarrow 0$.

Instead of solid body rotation of the flow in the cavity, the pressure drop is proportional to

$$\Delta p \sim (\rho \cdot \Omega^2 \cdot r_b{}^2 / 2) \cdot (1 - (r_a / r_b)^2) \qquad (2)$$

Here, as $r_a \rightarrow 0$, the cavity pressure drop Δp becomes a constant $\sim (\rho \cdot \Omega^2 \cdot r_b{}^2 / 2)$. Obviously, for a small ratio of exit to inlet radii, a simple free vortex has to be avoided.

3.2 Tubed vs. Tubeless Vortex Reducers

In aero-engines, this problem has been overcome by introducing vortex reducer systems. Vortex reducers are devices which counteract the free vortex effect by working as an (inefficient) turbine, taking swirl out of the air as it flows to smaller radii. Traditionally long hollow tubes have been used to achieve this.

However, the tubes are prone to vibrations due to the so-called “organ pipe effect“, which can introduce cracking due to high cycle fatigue. There are also restrictions in the length and the number of the tubes as the exit of the tubes cannot be allowed to touch each other or the disc faces. Tubed vortex reducer assembly can be very heavy and the flow through the tubes is very sensitive to the pressure ratio applied, potentially wasting precious compressor air.

Tubeless vortex reducers are an attractive alternative to the long straight tubes. The key feature of tubeless vortex reducers are deswirl nozzles, which are angled to produce a tangential velocity component of the air in opposite direction to the disc rotation. Thus the effective swirl of the air in the cavity downstream of the nozzles is reduced and the air leaves the cavity with a low angular velocity.

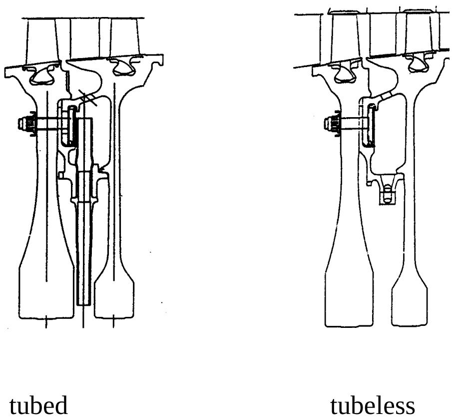

Fig. 2: Comparison of tubed vs. tubeless vortex reducers

The de-swirl nozzles are mechanically more robust and lighter than the tubed arrangements. Within the safe operating range the air flow through the tubeless vortex reducer is less sensitive to pressure variations than in the case of a tubed design. Fig. 2 shows a comparison of typical designs of tubed and tubeless vortex reducers.

Tubeless vortex reducer systems must be designed very carefully, since they feature a bi-stable mass flow characteristic at low pressure ratios. This can cause unstable operation. A transient breakdown of the tubeless vortex reducer system near the limit of stable operation has been observed in dedicated tests, which were performed during the engine development. Such a phenomenon can not occur with long tubed vortex reducer systems.

In the following the performance of both systems on the basis of rig and engine test data and 3-D CFD analyses is described and recommendations about the applicability of the tubed and tubeless vortex reducer systems in gas turbines are provided.

3.3 Vortex Reducers Theoretical Analysis

Despite the potential advantage of tubeless vortex reducers, to our knowledge, they are not used in aero-engines except in BR710 engines. As yet there is little information available in the public literature describing their performance. In the following we present a review of publications where the fundamental equations are derived and compared to generic experiments.

A review of the recent research on flows along discs with and without rotor-stator interaction as well as on radial flows between co-rotating discs has been published by M. Owen in 1988 [1]. Although the paper does not specifically address vortex reducer systems, it describes related phenomena as the Ekman-type boundary layers and the well known regions in cavities with radial in- or outflow, comprising a source region, where the incoming air mixes with the recirculating air, an
interior core of rotating fluid, and a sink region near the outlet.

A quite good understanding of radial flows between co-rotating discs can also be gained from the numerical analysis performed by J. W. Chew [2], published also in 1988. However, purely on tubeless vortex reducer systems, only three publications [3-5] are available.

A theoretical approach to determine the flow characteristic of de-swirl nozzles / disc-cavity-systems has been outlined by J. W. Chew [3,4]. He developed a mathematical model, using the momentum -integral method. In [3], presented in 1988, he investigated the use of fins to reduce the pressure drop in a radial cavity with radial inflow. In a later study [4], issued in 1989, he replaced the simple fins by more sophisticated de-swirl nozzles. In the latter case he predicted a bi-stable flow characteristic for the nozzle/ cavity system. His theoretical investigation has been experimentally validated by P. R. Farthing [4] in 1989.

P. R. Farthing has built up a large scale rig, which he ran up to 2000 rpm. The de-swirl nozzles were kept straight and the nozzle axis was angled against the direction of rotation. The two straight co-rotating discs, with the radial nozzle mounted at the discs outer radius, created a rectangular cavity with radial inflow. By varying disc speed and pressure ratio he experimentally determined the through-flow characteristic of such a tubeless vortex reducer system. The tests were restricted to one basic geometry. Further parameter of interest are the size and the shape of the nozzles, their radial position, their angle or the height to width ratio of the cavity were not varied. In so far, the validation of Chew's model was restricted to one rig set-up only.

Whereas [4] was concerned only with the pressure drop across the cavity, an extended study by Farthing and Owen [5] took also account of the losses in the nozzles and provides theoretical models to determine the overall pressure loss in the system. It is shown that although the swirl pressure loss in the cavity could be reduced to virtually zero and the overall pressure drop in the nozzles and the cavity always exceeds the one associated with solid body rotation.

Chew's and Farthing's theoretical predictions agree qualitatively very well with Farthing's test data. However, due to the limiting nature of the momentum-integral method and the limited test data available, the model was not considered sufficient for an extended aero-dynamical optimisation of the complex 3-D vortex reducer flow system.

3.4 Tubed Vortex Reducer Flow Equations

The prediction of the pressure losses in tubed vortex reducer flow systems is fairly straight forward. Fig. 2 shows a tubed vortex reducer where the flow path from the compressor off-take to the exit between the disc bores is broken down in regions A-E. The flow pattern in each region can be classified as :

A ➔ B: Free vortex
B ➔ C: Cross flow effect at pipe inlet
C ➔ D: Pipe losses, forced vortex
D ➔ E Pressure losses at the pipe exit
E ➔ F: Free vortex

The equations governing the non-isothermal incompressible free vortex flow (e.g. in the passage A ➔ B) are more complicated than the simple relationships derived in section 3.1 for isothermal flow. They are derived by noting that total pressure and temperature do not change across a free vortex and assuming isentropic relationship between pressure and temperature. The exit pressure and temperature have to be calculated numerically.

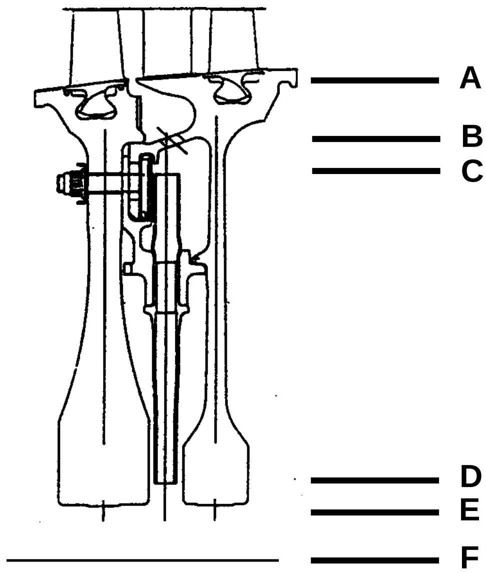

Fig. 3: Modelling of flow in tubed vortex reducer system

$$T_B = T_A \quad (3)$$

$$P_B = P_A \quad (4)$$

$$V_{W,B} r_B = V_{W,A} r_A \quad (5)$$

$$t_B = T_B - \frac{V_{W,B}^2}{2c_p t_B} \quad (6)$$

t_B is iteratively calculated with the energy equation

$$p_B = P_B * \left(\frac{t_B}{T_B} \right)^{\frac{\kappa}{\kappa-1}} \quad (7)$$

In the region C ➔ D, where the flow is characterised by a forced vortex, equation (5) has to be replaced by

$$V_{W,C} = \Omega r_C \quad \text{and} \quad V_{W,D} = \Omega r_D \quad (8)$$

The change in the fluid enthalpy from B➔ E can be calculated using the Euler equation:

$$a_v\,|_{adiabatic} = \Omega\left(V_{W,E} r_E - V_{W,B} r_B\right) \qquad (9)$$

a_V can be related to the enthalpy change Δh from steady state energy equation:

$$\Delta h = c_p (T_E - T_B) \qquad (10)$$

The pressure losses at entry and exit of the tubes and the pipe pressure losses are calculated using standard correlations.

The flow characteristics mass flow vs. driving pressure of the tubed vortex reducer system for long tubes spanning most of the radius resembles a simple restrictor characteristic. However, the point of zero mass flow is shifted to a driving pressure which is equal to the radial equilibrium pressure of the forced vortex in the vortex reducer tube.

A reduction in length of the tubes is often necessary in practical applications, diminishing the benefit of the system. In this case it may be useful to introduce protrusions or paddles into the regions upstream and / or downstream of the tubes to force the flow away from a free vortex towards a mixture of free and forced vortex (known as "Rankine vortex" in the literature).

3.5 Tubeless Vortex Reducer Characteristic

The flow characteristic of the tubeless vortex reducer is more complex due to the interaction of mean flow and boundary layers downstream of the vortex reducer nozzles. The equations for isothermal flow are derived in [2-4], but have to be solved numerically even in the isothermal case.

The main characteristics of the tubeless vortex reducer system is an s-shaped multi valued curve of mass flow vs. pressure ratio. The characteristics of tubed and tubeless vortex reducer systems are shown in fig. 4.

The characteristic to the left corresponds to a tubed vortex reducer. The s-shaped characteristic in the middle represents the tubeless system. Also shown is a typical flow characteristic of the air system flow path between vortex reducer exit and delivery to the

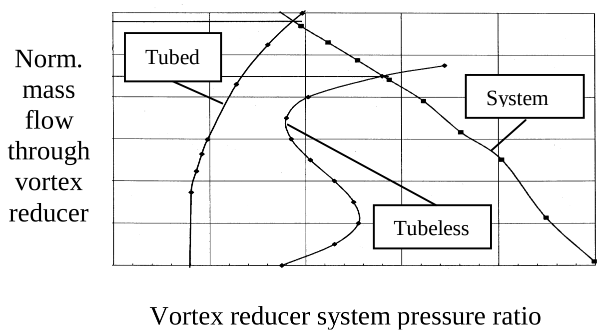

Fig. 4: Vortex reducer system flow characteristics

back of the HP turbine (to the right). The mass flow through the system is determined by the intersection of the vortex reducer characteristic and the flow characteristic of the remaining system.

3.6 Tubeless Vortex Reducer Qualification

Since the theoretical predictions were published and validated only for isothermal flow, they were considered not sufficient for the application of a tubeless vortex reducer into an aeroengine and the optimisation of the design. To qualify the tubeless vortex reducer system for application in the BR710 engine, numerous rig tests were carried out on a rig originally designed for application in the V2500 engine.

Tubeless vortex reducers featuring a variety of different design parameters were characterised in the rig tests and optimised for the application. The main parameters in the rig tests were a variation of the nozzle shape and effective area, the radial position relative to inlet and exit, pressure ratio across the cavity and speed of rotation. The vortex reducer designs used in the V2500 rig were scaled linearly from BR700 to V2500 dimensions.

The following paragraph describes the results of these rig tests and provide an explanation of findings.

4 Tubeless Vortex Rig Test Results

The angled nozzles in the ring which form the tubed design reduce the angular momentum of the inward flowing air, because the nozzles

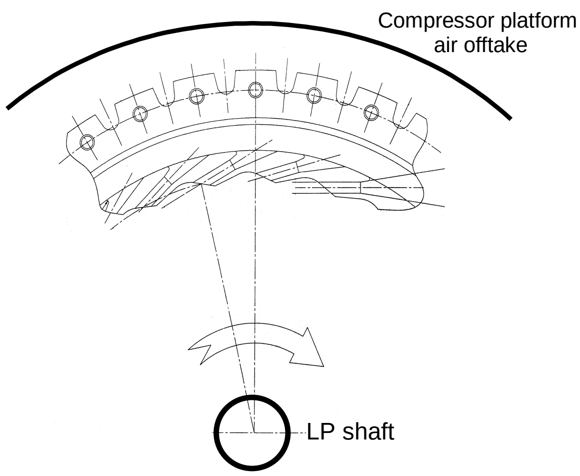

Fig. 5: Schematic view of tubeless vortex reducer

feed air into the inner cavity with an opposite whirl velocity relative to the drum. A view of a typical tubeless design is shown in fig. 5.

The flow and pressure losses in the cavity upstream and outboard of the de-swirl nozzles are fairly well predictable (the prediction follows the analysis for the flow upstream of a tubed vortex reducer, path A ➔ C in fig. 3).

In contrast, the flow in the inner cavity downstream of the nozzles is quite complex. Due to the frictional drag of the discs air is pumped outwards along the disc faces, creating a recirculating flow. The outward flow mixes with the de-swirled flow from the nozzles. The effective air whirl velocity V_W in the inner cavity is therefore the result of combining air from the nozzles with low negative whirl velocity and air entrained by the discs with high positive whirl velocity. It is mainly the effective swirl ratio $C_{eff} = V_{W,E} / \Omega * r_E$, which defines the flow field and the associated pressure drop Δp in the cavity downstream of the nozzles.

Fig. 6 shows the typical s-shaped mass flow characteristic of tubeless vortex reducer systems and the regions with over- and underswirl downstream of the vortex reducer.

The smallest pressure drop is achieved if the effective swirl ratio downstream of the nozzles is zero (upper knee). In this ideal case the air from the nozzles streams directly radial

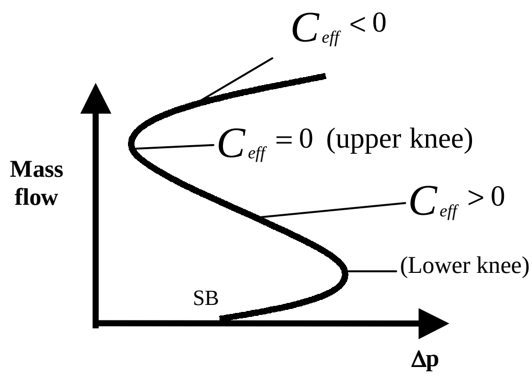

Fig. 6: Flow regimes of tubeless vortex reducer

inwards and accordingly the pressure drop cause by swril across the cavity becomes zero.

If the nozzle mass flow increases (above upper knee) and so its momentum (negative direction), it will dominate the mixing process with the entrained flow rotating in positive direction. As a consequence of that, the effective swirl will be negative and a vortex will establish, turning also into the negative direction. This will cause a pressure drop across the cavity. In theory, for extremely high mass flows, the pressure drop could become even infinity.

If the nozzle mass flow decreases (below upper knee), the entrained flow will dominate the mixing process and thus the resulting effective swirl will be positive. Due to the created vortex, turning now in positive direction, an associated pressure drop across the cavity will occur. If the mass flow further decreases frictional effects from the discs will more and more affect the vortex strength and limit the pressure drop to a certain maximum

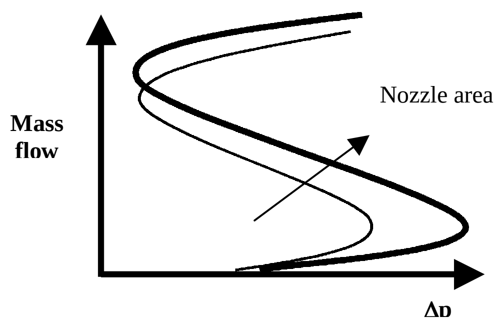

Fig. 7: Tubeless vortex reducer flow function: Effect of nozzle area

(lower knee). Finally, for virtually zero mass flow, the pressure drop will be defined by solid body rotation (marked SB in fig. 6).

The main means to tune such a system are nozzle angle, nozzle flow area and outer radius of the cavity downstream the nozzle size (mostly the inner radius is fixed by the shaft diameter). Increasing the flow area shifts the knees to higher mass flows and the lower knee also to the right (Fig. 7). That is due to the changed ratio between higher momentum of the flow from the nozzle to momentum (inertia) of the entrained flow. A similar effect becomes evident if the outer radius of the cavity is increased (Fig. 8). Fig. 9 shows the change in the characteristic due to rotational speed.

It is worth noting that only a tubeless vortex reducer with its nozzles directed against the direction of rotation of the disc can feature a S-shaped characteristic with three legs. For nozzles with radial or positive direction only the lower two legs can appear.

5 Application in BR700 Aeroengine

5.1 Air system design requirements

The predicted life of the turbine discs depends heavily on their internal temperature field. Hence an ingestion of hot gas from the main gas path to the disc faces can adversely effect the disc life. Consequently, the designer of the secondary air system has to make sure that the probability of undetected hot gas ingestion into the turbine cavities is extremely remote.

To apply a secondary air system with tubeless vortex reducers safely, the available pressure ratio has to be high enough to operate the system outside the multi-stable region. The operating point of the system has always to be on the upper leg of the characteristic (fig. 6), sufficiently far away from both knees of the s-shaped curve.

The available pressure ratio across the vortex reducer system varies on the operating line of the engine and is mainly a function of the aerodynamic speed NH/√T. The details of the curve depend on the characteristics of the pressure build-up in the compressor up to the air offtake to the vortex reducer system and on the reduction of pressure across the HP turbine.

In case of the BR700 engines the available

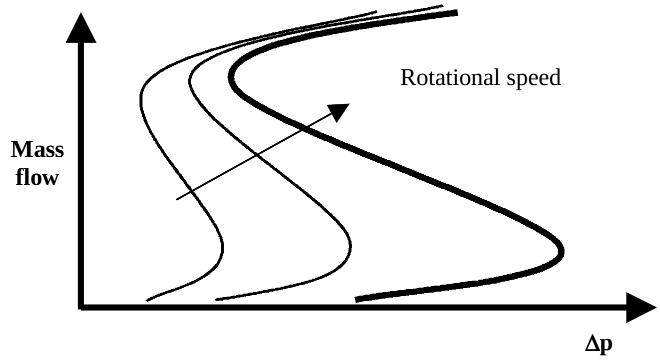

Fig. 9: Tubeless vortex reducer flow function: Effect of rotational speed

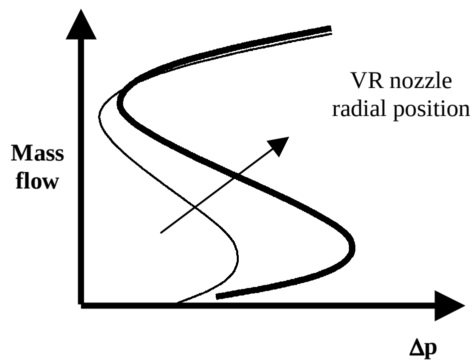

Fig. 8: Tubeless vortex reducer flow function: Effect of inlet radius

pressure ratio shows a maximum between 90 and 95 % aerodynamic speed. Above that, the pressure ratio drops towards higher speeds. Fig. 10 shows the pressure ratio for the BR710 and BR715 engines together with the breakdown limits of tubeless vortex reducer. The available pressure ratio in the BR715 engine is significantly higher than in the BR710 engine. The reason for this is the LP compressor (booster), which is present in the BR715 engine but not in the BR710. The offtake station of the air system in the HP compressor is the same in both engines.

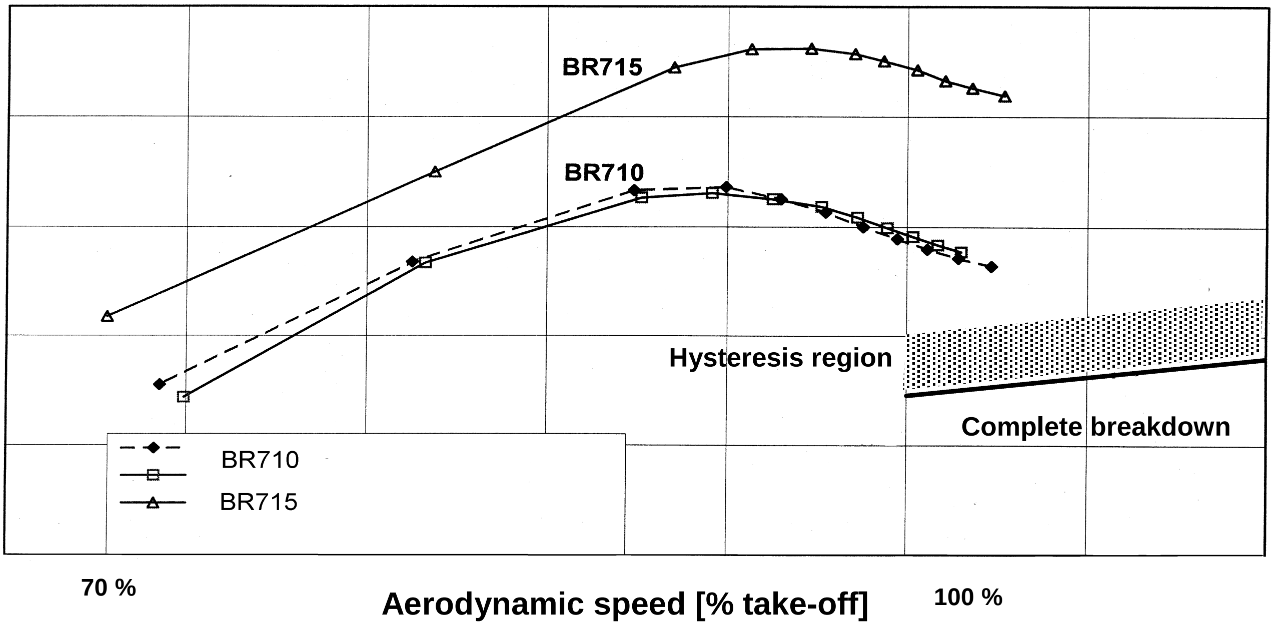

Fig. 10: Vortex reducer available pressure ratio as function of aerodynamic speed NH/√T

To ensure that a breakdown of the air system cannot occur in service, during the design and validation phase of the engine development a comprehensive failure mode and effects analysis (FMEA) has to be performed. The available pressure ratio has to be examined in the whole flight envelope and under all permissible flight conditions. The aerodynamic speed is influenced by Mach number, ambient pressure and temperature.

In addition, the FMEA has to take into account all potential tolerances and failures of the engine, which can affect the functional relationship between aerodynamic speed and available pressure ratio. Examples are compressor handling bleeds, customer bleeds, compressor variable guide vane schedule, rupture of pipes from the compressor casing, tolerance of turbine capacity and other factors. Combinations of these events, which are not of extremely remote probability, have to be taken into account in the analysis as well.

5.2 Transient behavior of tubeless vortex reducer system

On some development engines, which were modified to reach very high aerodynamic speeds outside the normal operating range, a hysteresis phenomenon of the air system with tubeless vortex reducers could be observed.

During slam accels to high power the temperature sensor in the cavity at the rear of the second stage HP turbine disc started to increase quickly, indicating hot gas ingestion. The temperature recovered to normal air system temperature after a delay time varying between the fraction of a second and several minutes. This delay time becomes longer as one approaches the line of breakdown, where it approaches infinity.

Fig. 11 shows a typical example of the time history of the cavity gas temperature during a slam accel to a aerodynamic speed very near to the breakdown limit. Also shown is the temperature of the main gas path and the speed of the HP shaft.

No such hysteresis effect has been observed with tubed vortex reducers. When using a tubeless vortex reducer system, one has to make sure that the region of hysteresis is outside of the operation range of the engine taking into account the relevant failure modes. A short transient temperature overshoot with remote probability might also be taken into account in the lifing of the turbine discs.

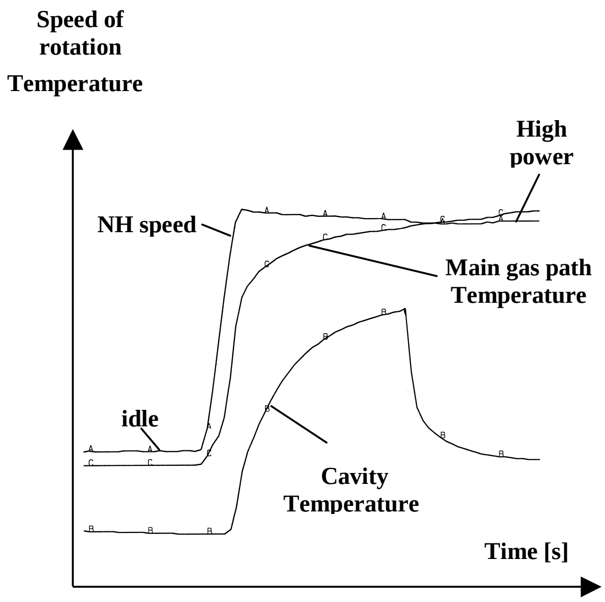

Fig. 11: Turbine cavity and main gas path temperature at slam accel to vicinity of breakdown line

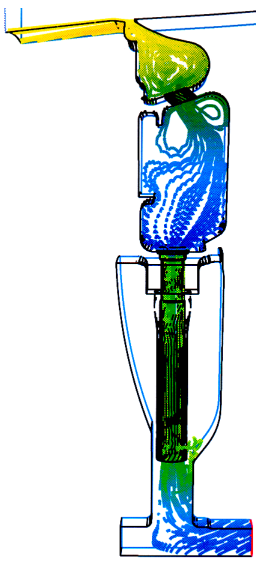

Fig. 12: 3-D CFD solution of tubed vortex reducer (streamlines colored by velocity)

6 CFD Validation and Optimisation

The process of design and development of a vortex reducer air system can be significantly improved if the flow characteristics and the pressure losses can be predicted with sufficient confidence. Although a wealth of rig test data was available for the design of the BR700 air system, it was felt desirable to have further support from CFD analysis for enhanced understanding of the flow physics and due to the high cost and large time scale of additional rig tests.

An in-depth 3-D CFD analysis of several vortex reducer design configurations and details of the flow path was performed. The commercial CFD code FLUENT/RAMPANT was used. Details examined included the shape and width of the offtake slot from the compressor platform, the influence of protrusions like nutheads along the flow path, the shape of the tubeless and tubed vortex reducers, the shape of the disc bores and the flow passages to the rear of the stage 2 turbine disc. Fig. 12 shows an example of a 3-D prediction of the flow through a tubed vortex reducer configuration.

To demonstrate the validity of the CFD calculations, the predictions of the mass flow through the vortex reducer system were compared to results derived from the rig tests. Fig. 13 shows the comparison. Note that each point in the figure represents a separate CFD calculation. There is a good agreement between CFD predictions and rig results.

The CFD solution converged only very

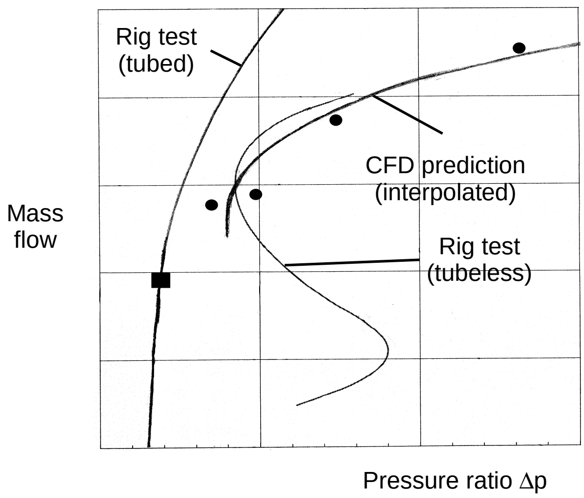

Fig. 13: Validation of CFD calculation with vortex reducer rig test results

slowly because of the low Mach numbers in the secondary air system cavities and the strong interaction of the main flow with the wall boundary layers. This is reflected in the scatter in the calculated mass flow from the CFD results. Using a prescribed pressure at the exit of the calculation domain, no solution on the lower parts of the tubeless vortex reducer characteristic could be obtained in agreement with the rig tests.

7 Summary and Conclusions

Two vortex reducer systems have been described. The systems are used to reduce the swirl in internal air passages of the secondary air system and avoid large pressure losses.

The tubed system is easier to understand and design, but has disadvantages of high weight and potential integrity problems. The mechanically more robust tubeless design has a more complex flow characteristic and more care is needed in the air system design for safe operation.

The steady-state and transient flow characteristics of both systems were described and compared to results from rig and engine tests. In particular, the hysteresis of the tubeless system was emphasized.

Many details of the system were optimised using the commercial 3-D CFD code FLUENT/RAMPANT and the application of the code to cavity flows was validated using results from the vortex reducer rig tests.

Both vortex reducer systems have been incorporated successfully into BR700 aeroengines

8 Acknowledgements

The permission from Rolls-Royce Deutschland for support of the work and permission to publish is gratefully acknowledged. Dr. J. Haarmeyer performed the 3-D CFD predictions of the vortex reducer systems. The discussions with D. Negulescu helped much to understand the flow physics of the vortex reducer system.

References

[1] M. J. Owen Air cooled gas turbine discs: A review of recent research. *International Journal Heat and Fluid Flow*, No 9, 1988, pages 354-365.

[2] 2. J. W. Chew, R. J. Snell Prediction of the pressure distribution for radial inflow between co-rotating discs. *ASME conference*, June 1988, Amsterdam. Paper-No.: 88-GT-61.

[3] 3. P.R. Farthing; J. W. Chew; J. M. Owen. The use of de-swirl nozzles to reduce the pressure drop in a rotating cavity with a radial inflow. *ASME Conference*, June 1998, Toronto. Paper No.: 89-GT-184.

[4] J. W. Chew, P. R. Farthing, J. M. Owen and B. Stratford. The use of fins to reduce the pressure drop in a rotating cavity with radial inflow. *ASME conference June 1988*, Amsterdam. Paper No.: 88-GT-58.

[5] P. R. Farthing and J. M. Owen De-swirled radial inflow in a rotating cavity, *Int. Journal of Heat and Fluid Flow*, Vol. 12, No. 1, March 1991.